DEUTSCHES ELEKTRONEN-SYNCHROTRON DESY

DESY 74/57
December 1974

Photoproduction and the Non-relativistic Quark Model

by

I. M. Barbour and R. G. Moorhouse
University of Glasgow, Glasgow, Scotland

W. A. Malone
Deutsches Elektronen-Synchrotron DESY, Hamburg

2 HAMBURG 52 · NOTKESTIEG 1

To be sure that your preprints are promptly included in the
HIGH ENERGY PHYSICS INDEX ,
send them to the following address (if possible by air mail) :

DESY
Bibliothek
2 Hamburg 52
Notkestieg 1
Germany

Photoproduction and the Non-relativistic Quark Model

by

I. M. Barbour and R. G. Moorhouse
University of Glasgow, Glasgow, Scotland

and

W. A. Malone[+]
Deutsches Elektronen-Synchrotron DESY, Hamburg

[+]European Exchange Fellow of the Royal Society.

1. Introduction

The photoproduction of pions has many features which are energy independent for incident photon energies greater than 3 GeV. For example, in charged pion photoproduction

$$\gamma N \to \pi^{\pm} N$$

$s^2 d\sigma/dt$ is constant at fixed t for $0 < -t < 1$ GeV^2; there is a forward spike and $\left(\frac{d\sigma}{dt}\right)_{\pi^-} = \left(\frac{d\sigma}{dt}\right)_{\pi^+}$ for $0 \leq -t \leq m_\pi^2$; away from the forward direction there is a marked change in the cross section ratios and

$$\left(\frac{d\sigma}{dt}\right)_{\pi^-} / \left(\frac{d\sigma}{dt}\right)_{\pi^+} \approx .35 \quad \text{for} \quad .2 < -t < .8 \quad .$$

Similar energy independent features are also observed in forward scattering for

$$\gamma N \to \pi^{\pm} \Delta$$

and in general there appear to be three distinct regions of t distinguished by the shape and slope of $d\sigma/dt$.

i) $0 < -t < m_\pi^2$
ii) $.2 < -t < .8$ GeV^2
iii) $1 < -t$ GeV^2

Attention has often been drawn to the aparently dominant role of pion exchange in region (i) (Refs.1,2); and indeed the data is in agreement with the contributions from either the electric Born approximation or the full Born approximation. However, away from this extreme forward direction, the data is in marked disagreement with the Born approximation, and other contributions must become important in the region (ii).

In an earlier paper (Ref.3), we have pointed out how a quark impulse approximation (Fig.1a) with the usual electromagnetic couplings of the quarks leads to an almost quantitative agreement with the observed π^+/π^- experimental ratios in region (ii). Of course, this impulse model alone is not sufficient to provide an explanation for the data. We have first to show that

1) the Born approximation dominates in region (i)
2) there exists some mechanism which will damp the Born terms at t increases
3) the contributions of the crossed graph (Fig.1b), which lead to charge ratios the inverse of Fig.1a, are suppressed.

A partial answer to the above points was provided by a fixed-dispersion relatic calculation (Ref.4), using knowledge of the low energy photoproduction amplitud (up to 1900 MeV) provided by Walker's analysis. The u-channel resonances correspond to the contributions of the crossed graphs (Fig.1b) and are distant from the physical region (ii) at high energy. Their contribution to the imaginary parts of the photoproduction amplitudes should therefore be zero. However, there is no a priori reason that the distant n-channel (and distant s-channel) resonances should not, via the dispersion relations, give large contributions to the real part. The above calculation showed that there was a strong cancellation between the Born terms and the contributions of the low-energy s- und u-channel resonances to the real parts. Furthermore the calculation indecated that this unidirectional cancellation obtained in the region $.2 < -t < .8$ GeV^2 whereas the resonance contributions, aside from the $\Delta(1236)$, were small compared to the Born terms in the extreme forward direction.

It is the purpose of this paper to try to extend the analysis in a model dependent fashion beyond the third resonance region, and to investigate the mechanisms governing this striking cancellation between the contributions of the low- and medium-energy resonances and the Born terms in the dispersion relations, should this continue.

The model we have chosen is the non-relativistic symmetric quark harmonic oscillator model. Calculations by Faiman and Hendry (Refs.6,7) and by Copley, Karl, and Obryk (Ref.8) show remarkable agreement between the harmonic oscillator model and experimental values for the low energy helicity amplitudes

2. Calculation

Basically the imaginary part of the amplitude is taken as given by Fig.1a, summed over all intermediate excited states. The lowest states, that is the nucleon and Δ in the 56 $n = \ell = 0+$ representation, must be treated differently, since they have all three quarks spatially unexcited, and the impulse approxi-

mation does not apply. The nucleon is inserted through the Born terms (Fig.2), and the Δ is taken from Walker's analysis. The non-relativistic limits of the hamiltonians relevant to the s-channel Born term specify the sign of the couplings of the quark amplitudes. The strong and electromagnetic decay widths of the Δ specify their magnitudes. The higher resonances, considered as excited three-quark states, appear in a zero-width approximation.

The individual members of the 70 $n = \ell = 1^-$ and 56 $n = \ell = 2^+$ can be calculated straight-forwardly using the wave-functions and hamiltonians of Faiman and Hendry (Ref.6). Their contribution via ReA to the cross section $d\sigma_\perp/dt$ is shown in Fig.3, where it can be seen that they tend to cancel the (Born $+\Delta$) term in the region $.3 < -t < .8$ GeV^2, confirming the earlier calculation. However the amplitudes calculated for these representations do not show the ratio π^+/π^- of 2:-1 of Refs.3 and 4, which were to produce a cross section ratio of 4:1, in the region $.2 < -t < .8$ GeV^2. In that model a sum over all intermediate spatial states was set equal to one, so that a cross section ratio could be obtained from the SU(6) part of the interaction. Here, however, following Faiman and Hendry, we have excluded certain intermediate states, namely the "spurious" ones, such as the 56 $\ell = 1^-$, whose wave-function is proportional to a centre-of-mass oscillation, and is not an excitation of the ground state. Indeed if one adds the contribution of the 56 $\ell = 1^-$ to the 70 $\ell = 1^-$ one recovers the 2:-1 ratio for π^+/π^-. The reason that the original model included "spurious" intermediate states is that the hamiltonian, proportional to $\exp(i\underline{k}\cdot\underline{r}_{(3)})$ where $\underline{r}_{(3)}$ is the position coordinate of the third quark, contains a dependence on the centre-of-mass coordinate $\underline{R} = \sqrt{3}^{-1}(\underline{r}_1 + \underline{r}_2 + \underline{r}_3)$, and thus produces spurious states.

We now wish to extend consideration to intermediate states belonging to higher representations $(\underline{\alpha}\ \ell\kappa)$ of total energy $(m+n\omega)$, where $\underline{\alpha}$ is 70 or 56 and the radial quantum κ is defined by

$$n = (\ell + 2\kappa) \quad .$$

If Θ is the angle between the photon and pion directions, the contribution of a representation $(\underline{\alpha}\ \ell\kappa)$ to the imaginary part of an helicity amplitude is

$$\mathrm{Im}\, A_{\mu\lambda} = \sum_{\psi} \{\langle\mu|H_s|\psi\rangle\langle\psi|S_E|\lambda\rangle\, d^q_{\mu\lambda}(\Theta) d^\ell_{oo}(\Theta)$$

$$+ \langle\mu|H_s|\psi\rangle\langle\psi|O_E|\lambda\rangle d^q_{\mu-1\lambda}(\Theta) d^\ell_{1O}(\Theta)\ \}$$

where q is the quark-spin involved; H_s the strong, and O_E and S_E the orbital and spin parts, of the electromagnetic hamiltonians respectively; and $\mu = \lambda_N - \lambda_\pi$, $\lambda = \lambda_N - \lambda_\gamma$. The states ψ are the members of the representation $(\propto \ell\kappa)$. $(\underline{56}\ \ell\kappa)$ is spanned by the states $\chi^m_{\ell,\kappa}\ g_s$; and $(\underline{70}\ \ell\kappa)$ by the states $\chi^m_{\ell,\kappa}\ g_\rho$ and $\chi^m_{\ell\ \kappa}\ g_\lambda$; where g_s, g_λ and g_ρ are purely symmetric, λ-symmetric and ρ-symmetric spin unitary spin wavefunctions (see Ref.6). The spatial wavefunctions are

$$\chi^m_{\ell,k} = \phi^{m_1}_{\ell_1 k_1}(\rho)\phi^{m_2}_{\ell_2 k_2}(\underline{\lambda})\ \phi^o_{o,o}\ (\underline{R})$$

with

$$m = m_1 + m_2$$
$$\ell = \ell_1 + \ell_2$$
$$k = k_1 + k_2$$

and $\phi^m_{\ell,k}\ (\underline{x})$ is an oscillator in the co-ordinate $\underline{x}$ with radial quantum number k, orbital momentum ℓ, third component m. By allowing only the ground-state oscillator in $\underline{R}$, we have excluded all spurious states; in matrix elements this is replaced by exp $(i\underline{P}\underline{R})$ and produces a δ-function for conservation of momentum. Strictly speaking the equation for ℓ should be interpreted as a vector coupling of $\underline{\ell}_1$, and $\underline{\ell}_2$ to make $\underline{\ell}$. However as we shall sum over all ℓ, we may use the simpler scalar equation, which is equivalent to a (negligibly) different cut-off (by the condition $[m+n\omega]^2 \leq s$), where ω is the level spacing.

The representations $\underline{\alpha}$ may be decomposed into submultiplets $\underline{\beta}$.

$$\underline{70} = (\underline{4},\underline{8}) + (2,\underline{10}) + (2,\underline{8})$$
$$\underline{56} = (4,\underline{10}) + 2,\underline{8})$$

On doing the algebra one obtains

$$\text{Im}\ A_{\mu\lambda}\ (\underline{\beta}\ \ell\ k) = a(\underline{\beta})\ S_1\ d^q_{\mu\lambda}\ d^\ell_{oo} + b(\underline{\beta})\ S_2\ d^q_{\mu-1\lambda}\ d^\ell_{10}$$

where a and b are independent of ℓ and k, and for the $\underline{70}$

$$S_1 = 4\pi gkf \sum_{\substack{\ell_1+\ell_2=\ell \\ K_1+K_2=K}} C_{\ell_1}^{K_1} C_{\ell_2}^{K_2} 3^{2K_1+\ell_1} Z_{\ell_1 K_1}$$

$$S_2 = 8\pi \frac{\alpha^2}{k} f \sum_{\substack{\ell_1+\ell_2=\ell \\ K_1+K_2=K}} C_{\ell}^{K_1} C_{\ell}^{K_2} 3^{2K_1+\ell_1} Z_{\ell_1 K_1}$$

$$\cdot \{\sqrt{\ell_1(\ell_1+1)} + \sqrt{\ell_2(\ell_2+1)}\}$$

where k and q are the photon and pion momenta in the C.M. frame; g is the quark gyromagnetic ratio (which we take as 1); α^2 is the spring constant; and

$$f = \left(\frac{kq}{24\alpha^2}\right)^{2K+\ell} \exp\left[-(k^2+q^2)/6\alpha^2\right]$$

$$C_{\ell_1}^{K_1} = (\ell_1 + 1/2)\{\Gamma(K_1+1)\,\Gamma(K_1+\ell_1+3/2)\}^{-1}$$

$$Z_{oo} = \{1 + (-1)^{\ell+1}\, 2^{2K+\ell}\}^2$$

otherwise

$$Z_{\ell_1 K_1} = \begin{cases} 1, & \ell_1 \text{ even} \\ 3, & \ell_1 \text{ odd} \end{cases}$$

The values of $Z_{\ell_1 k_1}$ are associated with the different normalisations $1/\sqrt{2}$ and $1/\sqrt{6}$ of $\underline{p}$-symmetric and $\underline{\lambda}$-symmetric states. Z_{oo} corresponds to the transition to the state symmetric in $\underline{r}_1$ and $\underline{r}_2$. For the $\underline{56}$ the result is similar. Each element in S_1, S_2 corresponds to a transition to one of the states $\chi^m_{\ell,k}$. The important point about these formulae is that the signs of S_1 and S_2 are independent of ℓ and k; thus for a fixed submultiplet $\underline{\beta}$, the contributions of $(\underline{\beta}\ \ell\ k)$ are all additive. This additivity leads to a problem. If one allows radial excitations, one finds that the ReA obtained from the dispersion relation completely swamps the Born term. We shall discuss this problem in the next section. Here we shall restrict attention to levels with

$n = \ell$, $k = 0$ which we call principal resonances.

In Figures 4,5, 7 we show the varying total contribution as n increases of the principal resonances to Re A_1 (A_1 largely detrmines the photoproduction cross-section at high energy). The contribution of the Born and Δ (i.e. the $n = 0$ representation) is given for comparison. Fig. 4 corresponds to the choice of a Regge type mass formula, Fig. 5 to the insertion of the average observed mass of the lower multiplets, and Fig. 7 to a straight Harmonic Oscillator mass formula with $\alpha^2 = 0.11$. In this case

$$d^{\ell}_{1o}(0) = -\frac{1}{\sqrt{n(n+1)}} \quad P'_n(\cos\Theta)\sin\Theta$$

$$d^{\ell}_{oo}(0) = P_n(\cos\Theta)$$

Ignoring the pion mass, $\cos\Theta = 1+t/2q^2$

$$q = \frac{m_R^2 - m^2}{2m_R} = n\omega\,\frac{(2m + n\omega)}{2(m+n\omega)}$$

If $n\omega >> m$ then $q \sim n\omega/2$.

$$d^{\ell}_{1o} \sim \frac{1}{\ell} P'_n(1-Z^2/2n^2)\sin\Theta \qquad Z^2 = -4t/\omega^2$$

$$d^{\ell}_{oo} \sim P_n(1-Z^2/2n^2)$$

Then the relation (Ref. 9)

$$\lim_{n\to\infty} \frac{1}{n^m} P^m_n(1-Z^2/2n^2) = J_m(Z)$$

leads us t form reminiscent of the optical model

$$H_{\mu\lambda} = a(\beta)S_1\, d^{q}_{\mu\lambda} J_o(Z) + b(\beta)\, S_2\, d^{q}_{\mu-1\lambda} J_1(Z)$$

so that all higher representations have the same angular dependence. Indeed for some sufficiently high n we may expect the contributions of higher representations to be zero at some value of t. In fact one sees from Fig. 7

that this happens already by n = 2, at $-t = .15$ corresponding to the first zero of $J_o(Z)$ at $Z = 2.5$. The effect sets in so quickly because even at low n, if $n\omega << m$, then

$$q \sim n\omega$$

The mass spectrum of the principal resonances if $m_R \propto \ell$. However Regge trajectories suggest $m_R \propto \sqrt{\ell}$. We have therefore performed an ad hoc "Regge" calculation, replacing $m_R = m + n\omega$ by $m_R^2 = m^2 + 2mn\omega$ (Fig. 4). The amplitude in the forward direction is then reduced, leaving (Born + Δ) free to give the experimental forward cross-section.

3. Remarks

We now try to show that some of the above mentioned properties are present in other models. We consider the spatial part of the electromagnetic hamiltonian S_E; this is associated with an incoming photon exp ($-i\underline{k}.\underline{r}$). We can expand the exponential:

$$\exp(-i\underline{k}.\underline{r}) = \sum_{\nu=o}^{\infty} i^{\nu} \sqrt{4\pi\,(2\nu+1)}\; Y_{\nu}^{o}(\Omega) \sqrt{\frac{\pi}{2kr}}\; J_{\nu+1/2}(kr)$$

If we can associate a $Y_{\ell}^{m}(\Omega)$ with the intermediate resonance state ψ - that is, if we adopt a composite model - conservation of angular momentum demands that only the term $\nu = \ell$ in the above sum be included. Thus after the angular integrations

$$\langle \psi \,/\, e^{-i\underline{k}.\underline{r}} \,/\, i \rangle = i^{\ell}\, 2\pi \frac{\sqrt{\ell+1/2}}{\sqrt{k}} \int_o^{\infty} dr\; f_{\ell,K}^{n}(r)\; r^{3/2}\; J_{\ell+1/2}(kr)\; f_{oo}^{o}(r)$$

where $f_{\ell,K}^{n}(r)$ is the spatial wavefunction associated with orbital angular momentum ℓ and the n^{th} energy level. At the strong vertex, linear momentum conversation demands an outgoing pion exp (+ $i.\underline{q}.\underline{r}$). As before we get:

$$\langle f \,/\, e^{i\,\underline{q}.\underline{r}} \,/\, \psi \rangle = (-i)^{\ell}\, 2\pi \frac{\sqrt{\ell+1/2}}{\sqrt{q}} \int_o^{\infty} dr\; f_{\ell K}^{n}(r)\; r^{3/2}\; \tau_{\ell+1/2}(qr)\; f_{oo}^{o}(r)$$

Thus the sign of the contribution to the amplitude, depending on the product of these two, is always the same. A somewhat similar argument holds for O_E. The only assumptions involved here are conservation of linear and angular momentum,

and the use of a composite model for the intermediate state, so that the argument is very general.

The expression of the amplitude as a sum of transitions to states is, within a shell model, perfectly general, and we may write formally

$$A = \sum_{\text{levels } n} \sum_{\ell+2K=n} \sum_{\substack{\ell_1+\ell_2=\ell \\ K_1+K_2=K}} A^{K_1K_2}_{\ell_1\ell_2}$$

where that $A^{K_1K_2}_{\ell_1\ell_2}$ are all positive, because of the above argument. Now if we allow all possible radial excitations, where will be a very rapid increase in the number of terms in this series. If we write

$$A = \sum_{\text{levels } n} A^n = \sum_{\text{levels } n} \sum_{\ell+2K=n} A^{\ell,K}$$

then the number of terms in A^n is increased by a factor ~ n/6 if radial excitations are included. Further, if we consider the terms $A^{\ell,K}$ for a fixed n then it is reasonable to suppose that those terms with a low ℓ will be enhanced over those with large ℓ , by the angular momentum barrier effect familiar from elementary quantum mechanics; and the greater n, the greater this enhancement.

To improve this calculation, therefore, would require a shell-model potential with a very strong bias against high excited states or at least against highly excited radial states. The use of a more complicated Hamiltonian (than the exp {- ik.r}) does not appear to help. Although the simple argument above does not hold, for example, when one includes a pion recoil term as in Ref. 10, a calculation has shown that the same problem arises there. I should be noted that similar arguments to the above should obtain even for a "relativistic" shell model if the SU(6) part of the interaction can be treated separately from the spatial part as in Ref. 10.

4. Conclusions

We have shown that the simple quark impulse model for pion photoproduction that originally motivated this work is invalid, in that it obtained the charge ratio 2:-1 for the charged pion amplitudes by including spurious states. One could

re-interpret the model as impulse excitation of one of three valence quarks surrounding a heavy core, but this gives rise to more SU(6) representations than are yet seen, unless we assume that the valence-core picture is only valid at high energies.

The failure of the straight forward harmonic oscillator model at high energies, when radial states are included, is more serious. It seems that some states can only be accomodated in radially excited SU(6) representations e.g. the P_{11}(1470). (See Ref. 12 for details of others). On the other hand, this simple model predicts well signs and magnitudes of couplings in photoproduction at low energies (Ref. 13). But it is too facile to blame this on the harmonic oscillator potential, as section 3 shows; indeed the harmonic oscillator potential is merely the only analytically soluble shell model that we have. It seems to us that the (nonrelativistic) shell model itself is invalid at high energies; of course it is already puzzling that the baryon resonances should behave like non-relativistic three quark bound states at low energies.

Figure Captions

Fig. 1. a) Quark model diagram for pion photoproduction with s-channel excitation only.
b) Crossed diagram representing u-channel excitation only.

Fig. 2. Feynmann diagrams of Born approximation amplitudes for $\gamma N \to \pi^{\pm} N$

Fig. 3. The contribution to $(s-m^2)^2\, d\sigma/dt$ arising from the real parts of the high energy π^+ photoproduction amplitudes as evaluated using dispersion relations. The various curves represent the results as various resonances of the 70 $\ell=1^-$ and 56 $\ell=2^+$ representations are included in Im A.

Fig. 4. The amplitude A_1 which determines the cross-section for π^+ photoproduction around the forward direction. Shown is the contribution to $\mathrm{Re}A_1^{\pi+}$ of the representations $\ell=(2n+1)^-$ and $\ell=(2n)^+$ with K = 0, via dispersion relations. A "Regge" type mass formula $m_R^2 = m^2 + 2mn\omega$ was used.

Fig. 5. As Fig. 4., with harmonic oscillator mass-formula $m_R=m+n\omega$.

Fig. 6 Contribution to the cross-section of Born $+\Delta+\mathrm{Re}A^+$ of Fig. 4.

Fig. 7. As Fig. 5. but with $\alpha^2 = .11$.

References

1. B. Richter in "Preceedings of the Third International Symposium on Electron and Photon Interactions at High Energies, SLAC(1967)" p. 309; H. Harari, ibidem, p. 337.

2. N. Dombey, Physics Letters 30B, 646 (1969).

3. I.M. Barbour and R.G. Moorhouse, Nuclear Physics B20, 629 (1972).

4. Barbour et al., Phys. Rev. D4, 1521 (1971).

5. Walker, Phys. Rev. 182, 1729 (1969).

6. Faimann and Hendry, Phys. Rev. 173, 1720 (1968).

7. Faimann and Hendry, Phys. Rev. 180, 1572 (1969).

8. Copley, Karl and Obryk. Nuc. Phys. B8, 609 (1968).

9. Whiltaker and Watson, "Modern Analysis" (C.U.P. 1946) p. 367.

10. Feynman et al., Phys. Rev. D3, 2706 (1971).

11. Boyarski et al., Phys. Rev. Letters 20, 300 (1968).

12. Kim and Noz, Nuovo Cimento 11A, 513 (1972); Maryland University preprint 74-018.

13. Moorhouse and Oberlack, Phys. Lett. 43B, 44 (1973); Moorhouse and Parsons, Bonn Conference contribution and Nuc. Phys.

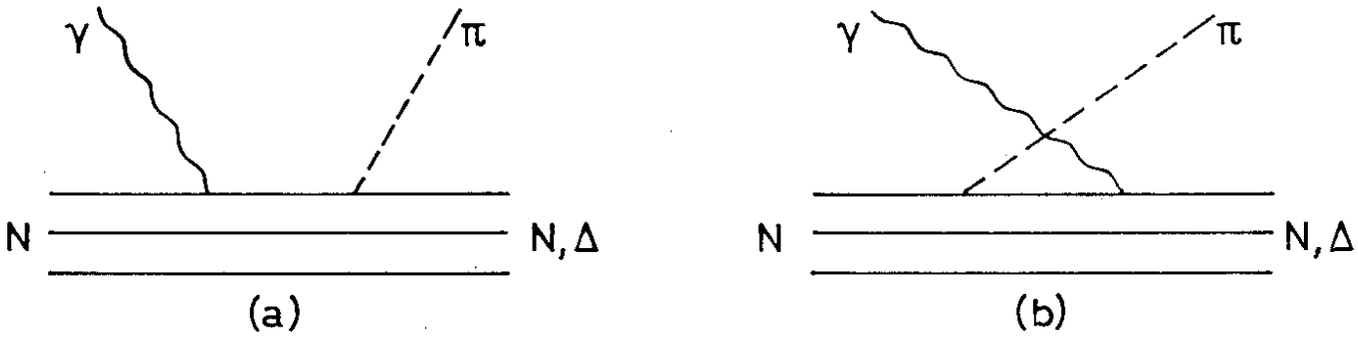

Fig.1

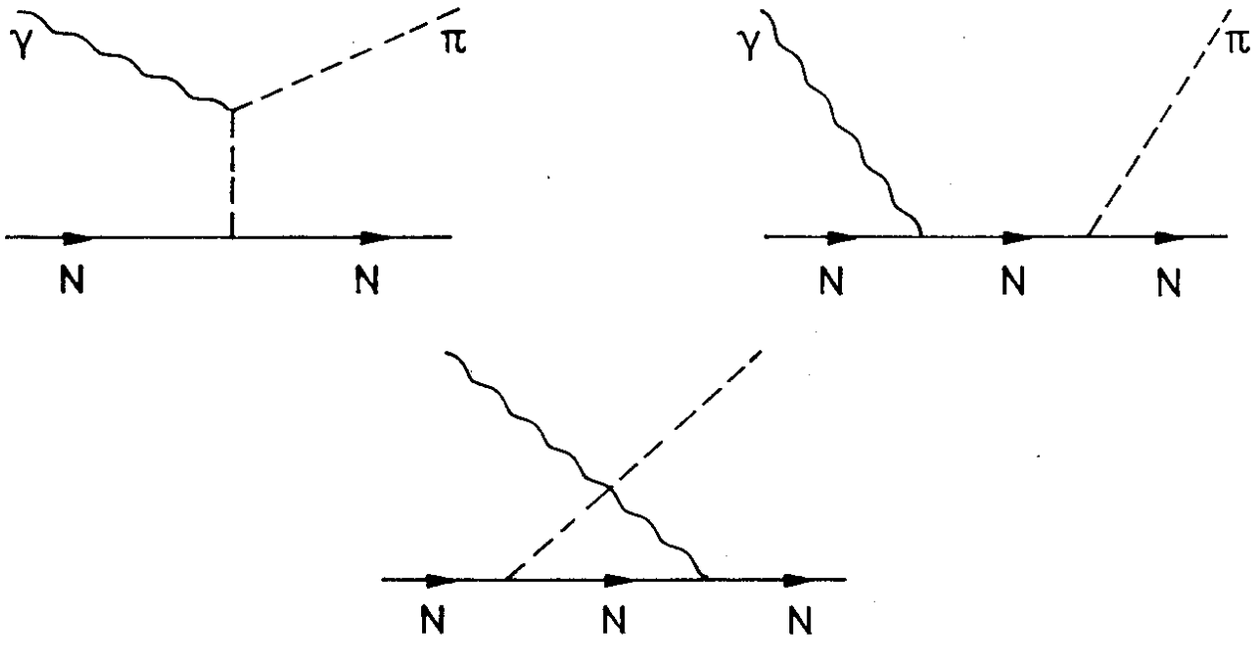

Fig. 2

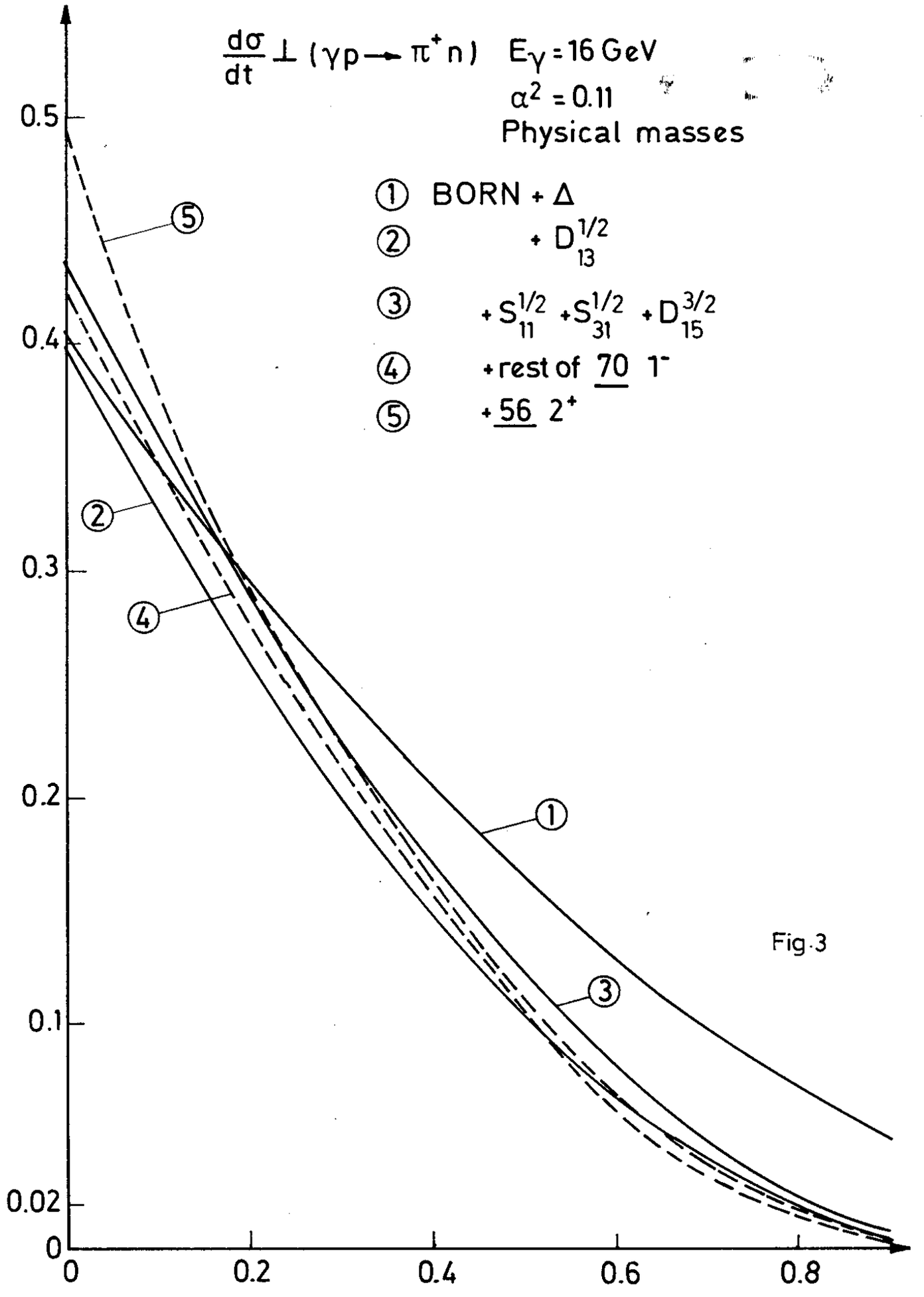
$\frac{d\sigma}{dt}\perp(\gamma p \to \pi^+ n)$ $E_\gamma = 16$ GeV
$\alpha^2 = 0.11$
Physical masses
① BORN + Δ
② + $D_{13}^{1/2}$
③ + $S_{11}^{1/2}$ + $S_{31}^{1/2}$ + $D_{15}^{3/2}$
④ + rest of 70 1^-
⑤ + 56 2^+
0.5
0.4
0.3
0.2
0.1
0.02
0
0
0.2
0.4
0.6
0.8

Fig.3

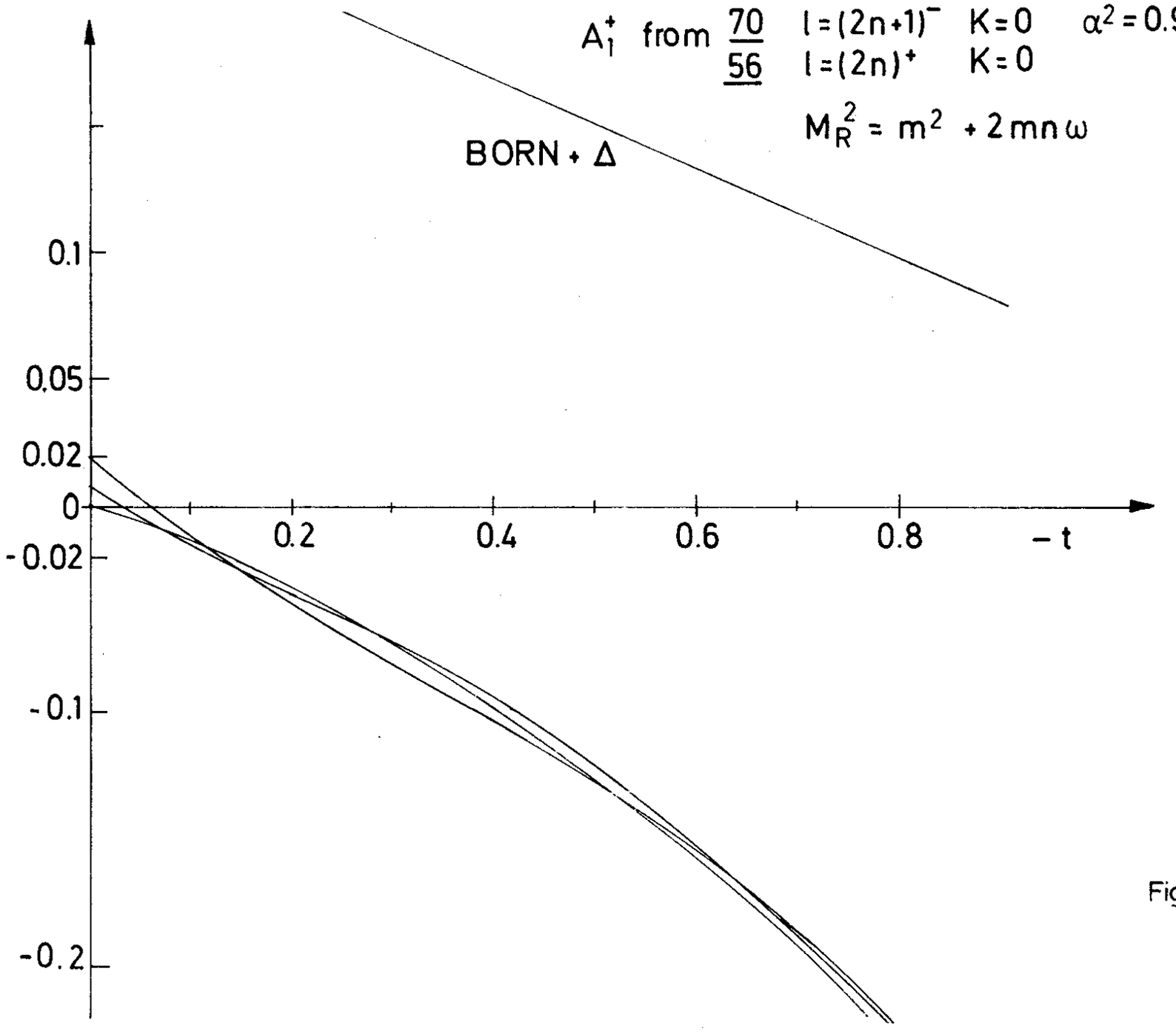
A_1^+ from 70 $l=(2n+1)^-$ $K=0$ $\alpha^2=0.9$
56 $l=(2n)^+$ $K=0$
$M_R^2 = m^2 + 2mn\omega$
BORN + Δ
0.1
0.05
0.02
0
-0.02
-0.1
-0.2
0.2
0.4
0.6
0.8
$-t$

Fig.4

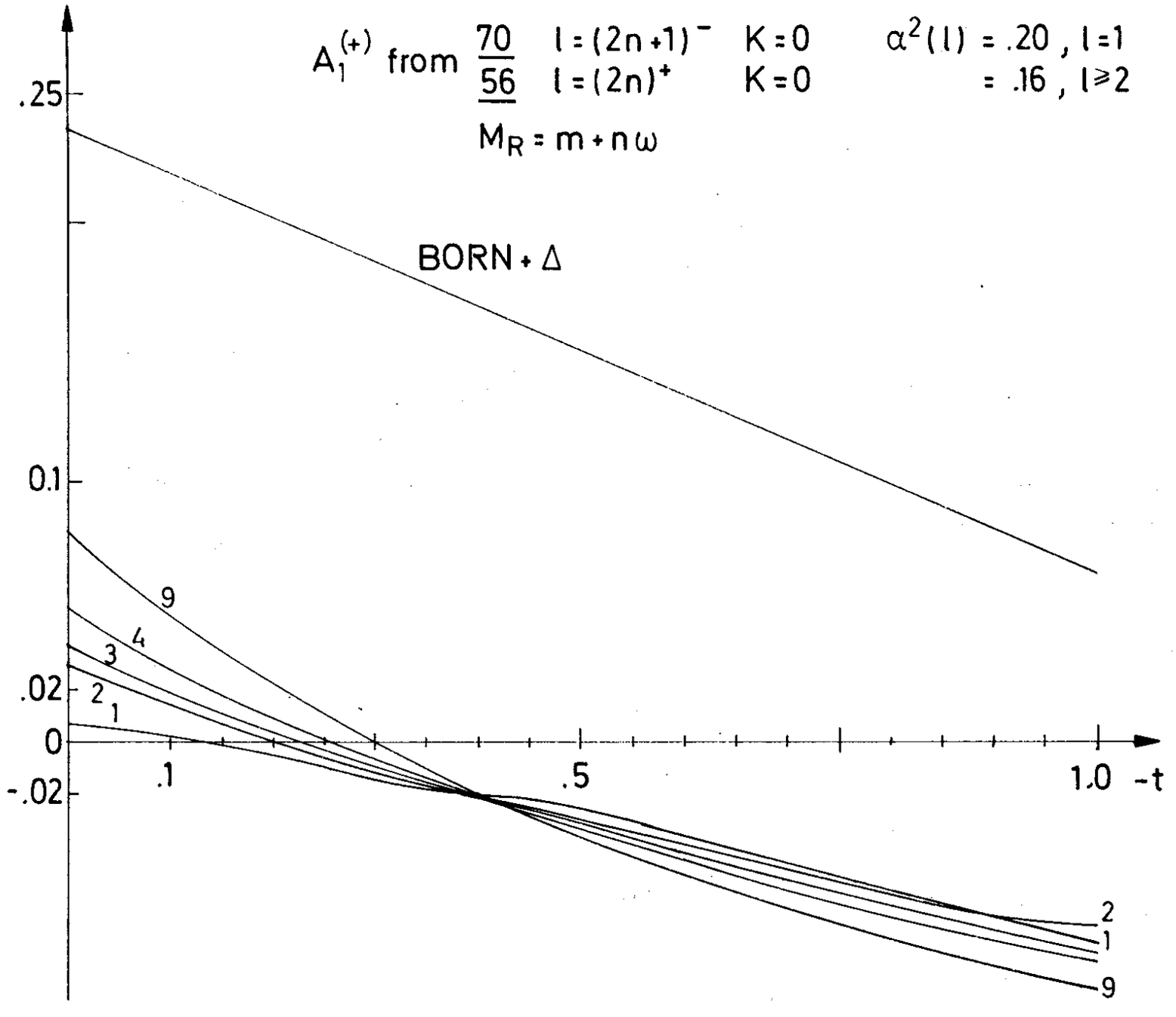
$A_1^{(+)}$ from 70 $l=(2n+1)^-$ $K=0$ $\alpha^2(l)=.20$, $l=1$
56 $l=(2n)^+$ $K=0$ $=.16$, $l\geq 2$
$M_R = m + n\omega$
.25
0.1
.02
0
-.02
BORN + Δ
9
4
3
2
1
.1
.5
1.0
-t
2
1
9

Fig. 5

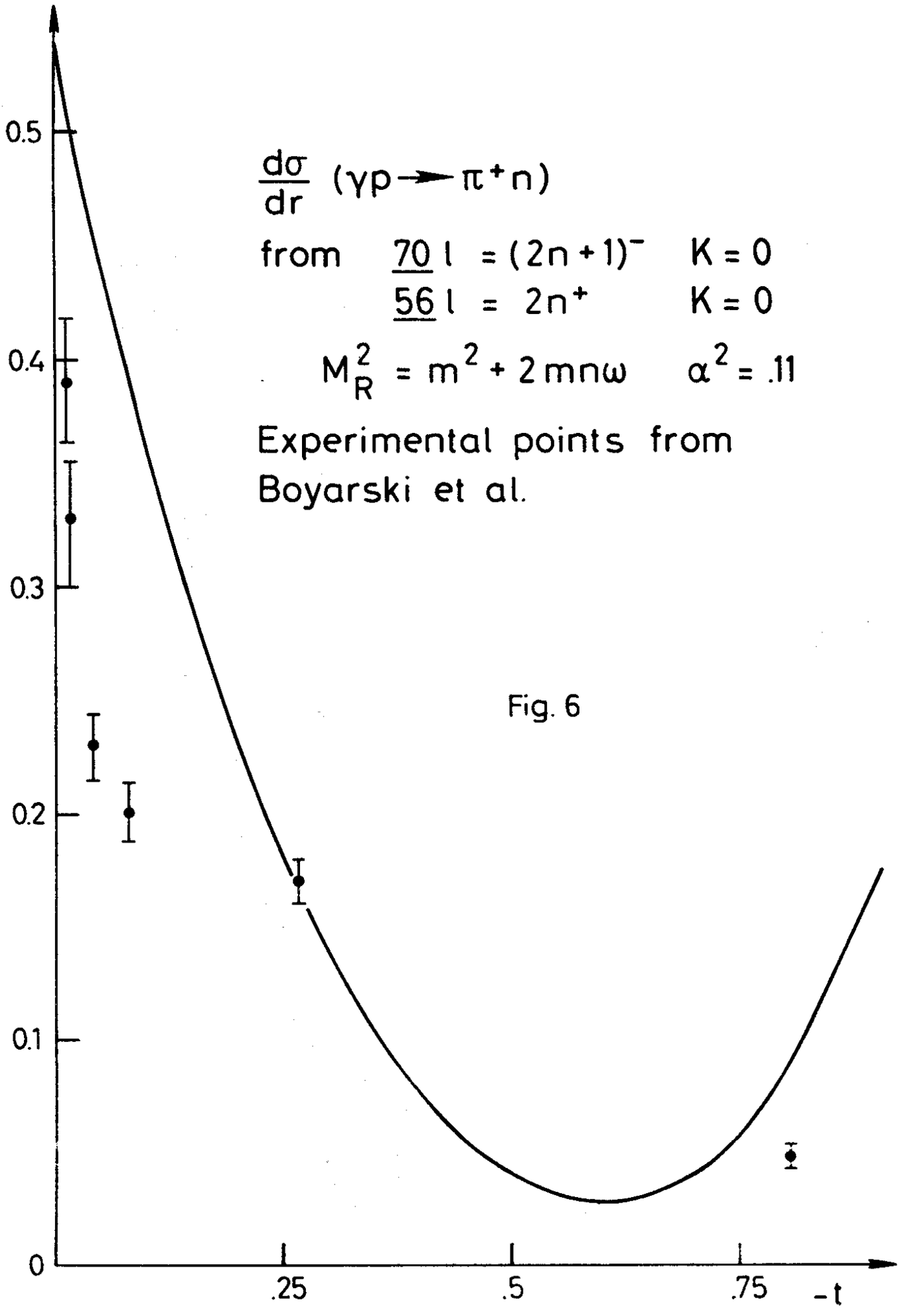
$\frac{d\sigma}{dr}$ $(\gamma p \rightarrow \pi^+ n)$
from $\underline{70}\ l = (2n+1)^-$ $K = 0$
$\underline{56}\ l = 2n^+$ $K = 0$
$M_R^2 = m^2 + 2mn\omega$ $\alpha^2 = .11$
Experimental points from
Boyarski et al.
0.5
0.4
0.3
0.2
0.1
0
.25
.5
.75
-t

Fig. 6

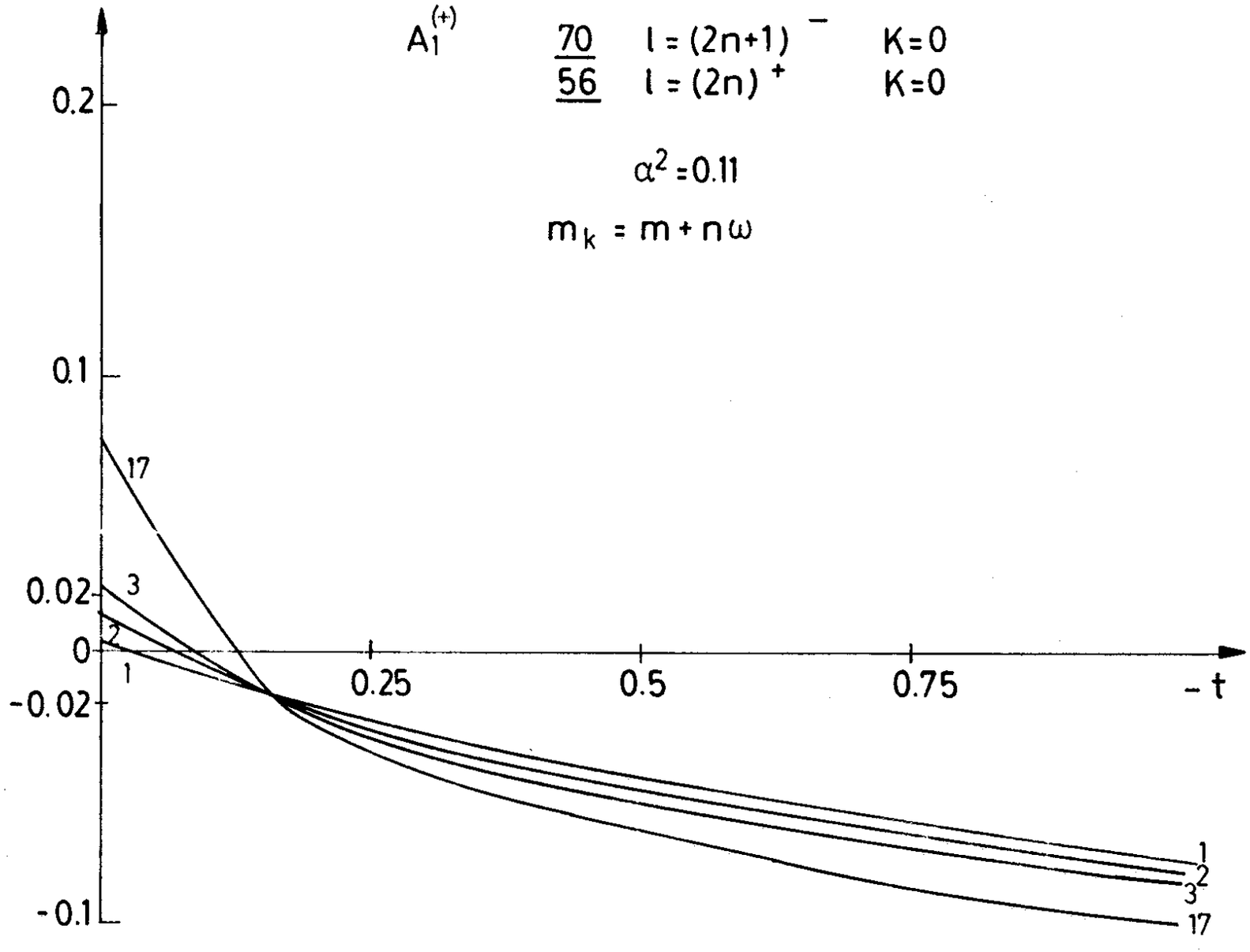
$A_1^{(+)}$
70 $l = (2n+1)^-$ K=0
56 $l = (2n)^+$ K=0
$\alpha^2 = 0.11$
$m_k = m + n\omega$
0.2
0.1
0.02
0
-0.02
-0.1
17
3
2
1
0.25
0.5
0.75
- t
1
2
3
17

Fig. 7